2004

A Holocene Record of Changing Arctic Ocean Ice Drift Analogous to the Effects of the Arctic Oscillation

Dennis A. Darby
Old Dominion University, ddarby@odu.edu

Jens F. Bischof

Original Publication Citation

Darby, D. A., & Bischof, J. F. (2004). A holocene record of changing Arctic Ocean ice drift analogous to the effects of the arctic oscillation. *Paleoceanography, 19*(1), PA1027. doi:10.1029/2003pa000961

A Holocene record of changing Arctic Ocean ice drift analogous to the effects of the Arctic Oscillation

Dennis A. Darby and Jens F. Bischof

Department of Ocean, Earth, and Atmospheric Sciences, Old Dominion University, Norfolk, Virginia, USA

Received 26 August 2003; revised 5 December 2003; accepted 22 January 2004; published 19 March 2004.

[1] The Arctic Oscillation (AO) controls the configuration of the Transpolar Drift (TPD). If thicker ice from the Beaufort Gyre were exported, the volume of fresh water/sea ice in the Nordic seas would significantly increase, decreasing the formation of North Atlantic deep water. This would cool large parts of the Northern Hemisphere and affect global climate. Therefore, in order to understand how the global climate system functions, it is imperative to know how the TPD changed over the last millennium or more. The provenance of grains in a sediment core located near the confluence of the TPD and the Beaufort Gyre provides a direct proxy for changes in seaice drift owing to these circulation systems. The core has more than 200 cm of Holocene sediment, with intervals dominated by grains from the Russian shelves alternating with intervals of abundant grains from North American sources. Grains matched to Russian shelves indicate that the TPD was shifted toward North America, similar to what occurs during a more positive phase of the AO. This condition alternated with intervals where few grains matched to Russian sources, presumably because the TPD was restricted to the Russian half of the Arctic, far from the core site. During the last 1300 years, increased influx of Russian grains occurred approximately every 50–150 years. This fluctuation might represent the long-term oscillation of the AO, which modulates the same TPD shift today. *INDEX TERMS:* 1620 Global Change: Climate dynamics (3309); 4267 Oceanography: General: Paleoceanography; 4558 Oceanography: Physical: Sediment transport; 3022 Marine Geology and Geophysics: Marine sediments—processes and transport; 9315 Information Related to Geographic Region: Arctic region; *KEYWORDS:* Arctic Ocean, ice rafting, climate change

Citation: Darby, D. A., and J. F. Bischof (2004), A Holocene record of changing Arctic Ocean ice drift analogous to the effects of the Arctic Oscillation, *Paleoceanography*, *19*, PA1027, doi:10.1029/2003PA000961.

1. Introduction

[2] The drift of ice in the Arctic Ocean varies primarily with changes in sea level pressure and resulting wind patterns. The Arctic Oscillation (AO) [*Thompson and Wallace*, 1998] explains most of the variance in sea level pressure and ice motion [*Rigor et al.*, 2002], and these variations in wind associated with the AO modulate the location of the transpolar drift (TPD) [*Mysak*, 2001; *Mysak and Venegas*, 1998; *Kwok*, 2000], the major ice drift system controlling ice export from the Arctic through Fram Strait. When positive, the AO induces the TPD to intensify, shifting farther eastward from Siberia toward North America. In addition to affecting ice conditions in the Arctic Ocean, this change in the TPD causes an increased export through Fram Strait of the thicker ice in the Beaufort Gyre [*Hilmer and Jung*, 2000; *Rigor et al.*, 2002; *Kwok and Rothrock*, 1999], reducing the surface salinity in the Greenland Sea, which subsequently diminishes the thermohaline circulation by slowing the production of NADW [*Aagaard and Carmack*, 1989; *Raymo et al.*, 1990; *Delworth and Dixon*, 2000]. This in turn has been linked to climate change initiating a cooling over northern Europe and eastern Canada [*Dickson et al.*, 1988]. When the AO is negative, the TPD is more restricted to the Russian Arctic, and the clockwise Beaufort Gyre dominates the Arctic Ocean near North America (Figure 1). The causes of these changes that generate the fluctuations in the AO and that correlate to fluctuations in the North Atlantic Oscillation (NAO) are yet to be established [*Dickson et al.*, 2000]. Even the nature of the oscillation is poorly confined and certainly its existence and frequency over more than the last half century are poorly understood despite attempts to replicate it statistically [*Luterbacker et al.*, 2001, and references therein]. This paper presents evidence that a changing ice drift regime has existed in the Arctic since the earliest Holocene and that it has multidecadal to century scale oscillation over the last millennium and perhaps longer.

2. Materials and Methods

[3] Piston core P1-92-AR-P1 (4.1 m length) and its companion box core P1-92-AR-B3 (0.42 m) (herein referred to as P1 and B3) are in an ideal location (73°42.40′N, 162°44.60′W) to record ice-rafting from Siberia due to a TPD shift toward Alaska (Figure 1). These cores, along with several others traversing the continental slope down into the Northwind Basin, were recently sampled and analyzed for several paleoenvironmental proxies as part of the NSF Western Arctic Shelf Basin Interaction Program [*Darby et al.*, 2001]. Box core B3 was sampled at every centimeter, and piston core P1 at every centimeter between 0–10 cm,

0883-8305/04/2003PA000961

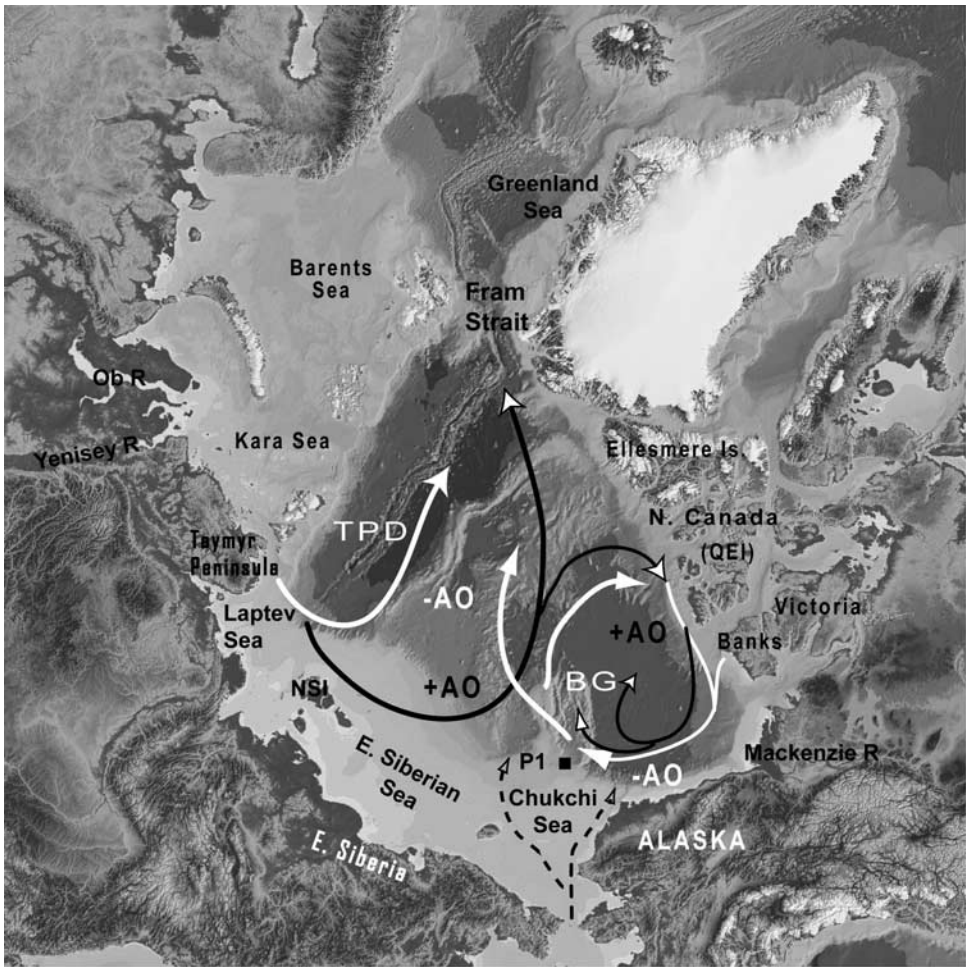

Figure 1. The modern Arctic ice drift pattern (white arrows) shows a fairly direct path of the transpolar drift (TPD) from the Laptev Sea to Fram Strait corresponding to a negative Arctic Oscillation (AO). When the AO is positive, the TPD shifts toward North America (black arrow) and the Beaufort Gyre (BG) diminishes. The Pacific ice drift through Bering Straits bifurcates across the Chukchi Sea (small dashed arrows), the eastern branch approximates the Alaskan Coastal Current and the western branch points toward Herald Canyon. NSI, New Siberian Islands; QEI, Queen Elizabeth Islands. See color version of this figure in the HTML.

and at 5 cm intervals below this depth, taking 2 cm thick samples. The lithostratigraphy in P1 is rather simple compared to deeper water cores in this and other parts of the Arctic Ocean [*Darby et al.*, 1997], and consists of olive gray mud with an average of 1.9% (0.6–5.2%) sand from the surface down to 229 cm core depth, where the sand content increases to an average of 8% (4–26%) below this depth. This change in sand content is generally considered the boundary between oxygen isotope stages 1 and 2, or the Holocene-Late Pleistocene boundary [*Phillips and Grantz*, 1997; *Poore et al.*, 1999; *Darby et al.*, 1997]. It marks the change from largely glacial iceberg rafting to primarily sea ice rafting in the Arctic at the last glacial termination. Sea ice rafting is indicated by low amounts of ice-rafted detritus (IRD) >63 μm, and by IRD sources from presently unglaciated shelf areas [*Darby et al.*, 2002]. The fine-grained, laminated sediment interval interpreted as the glacial maximum (18–22 ka) in nearby Northwind Ridge cores is absent [*Phillips and Grantz*, 1997].

[4] The chronstratigraphy of P1 and B3 was determined by AMS radiocarbon analyses on four mollusk or benthic foraminifer samples from B3 and seven similar but mostly mollusk samples from P1. The overlap in C-14 ages as well as a unique detrital dolomite peak in both cores was used to splice these cores. This indicated that 20 cm was missing from the top of P1. Approximately 5 cm is also missing from the top of B3 due to over-penetration of the box corer. This material, which extended above the top of the corer, was partly eroded as the core was retrieved and was not sampled by the push tubes inserted into the box core. Despite this missing material at the sediment water interface, P1 and B3 contain a detailed record of change during the deglaciation at the last glacial termination and the overlying Holocene [*Darby et al.*, 2001].

[5] The radiocarbon dates were corrected for the carbon reservoir effect by subtracting 450 years [*Forman and Polyak*, 1997; *Bauch et al.*, 2001a, 2001b]. There is no generally accepted reservoir correction for this part of the

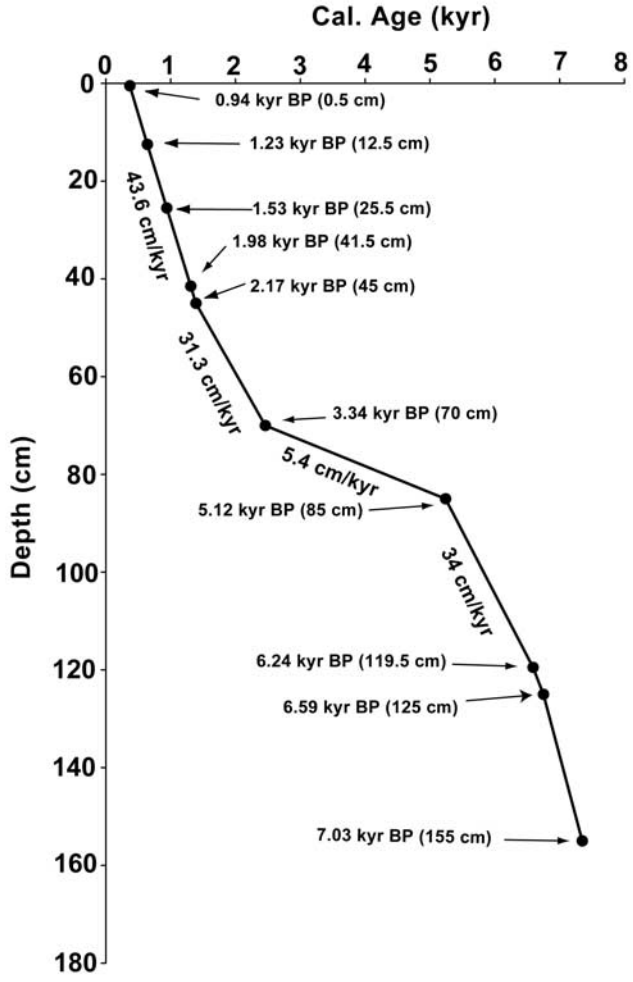

Figure 2. Age model for B3/P1 shows the changes in sedimentation rates. The uncorrected radiocarbon age dates are shown with the arrows.

Arctic Ocean and these ages might be somewhat younger if older carbon from the Pacific reaches the P1 site [*Kiefer et al.*, 2001; *Kennett and Ingram*, 1995; *Southon et al.*, 1990]. These ages were converted to calendar years using Calib.4.4 ($\Delta R = 50$) [*Stuiver and Reimer*, 1993; *Stuiver et al.*, 1998]. Interpolated ages were used to construct an age model for the cores where age and depth were linear (if $r^2 > 0.98$) or second order polynomial otherwise (Figure 2). Four segments of different sedimentation rates occur in the Holocene, with an overall average rate of 22 cm/kyr (Figure 2). The core top interval, 370–1300 years BP (where 0 years BP is 1950 AD) [*Stuiver et al.*, 1998] has a uniform sedimentation rate of 44 cm/kyr, but the interval between 2.5 and 5.3 ka has much lower rates. The sedimentation rates during the early Holocene of 31.5 cm/kyr might be even higher during the peak of the deglaciation following the Younger Dryas (11 ka), so the bottom of the core might be somewhat younger than extrapolation would indicate. Since the large ice sheets that calved into the Arctic Ocean disappeared by 10 ka [*Dyke*, 1987] and the last large spike in Fe oxide detrital grains traced to the Arctic Laurentide Ice Sheet in a core from Fram Strait declines between 12.2 and 11 ka [*Darby et al.*, 2002], the extrapolated age for the rapid decline in IRD in P1 at 9.5 ka is reasonable.

[6] All samples were wet-sieved at 45, 63, 125, and 250 μm. Fe oxide grains were magnetically separated (Franz magnetic separator) from the 45–250 μm fractions and mounted in clear epoxy plugs, whose surface was ground to expose cross sections of the grains, then polished. Nine different Fe oxide mineral types were identified by reflected light microscopy (1000X) and confirmed by chemical composition (microprobe analyses). Both the clay (<2 μm) and silt (2–63 μm) fractions mineralogic content were determined by X-ray diffraction (XRD) using smear slides and standard techniques [*Reimnitz et al.*, 1998]. The general accuracy on these clay mineral abundance estimates is approximately 25% of the value, based on similar analyses of clay standards. The >250 μm fraction was analyzed quantitatively under a binocular microscope for lithologic and mineralogic composition, using a classification scheme that consists of more than 300 categories. These are combined into 72 lithic types, of which less than 15 are generally abundant. If available, at least 300 and up to 600 grains are counted for a statistically useful sample.

[7] Our method of source determination of ice rafted debris is described in detail in the work of *Darby and Bischof* [1996] and updated in the work of *Darby* [2003]. In order to determine whether a grain assemblage >250 μm (lithic IRD) or a single, opaque Fe-oxide mineral is from a particular circum-Arctic source, we first established a reference database of more than 300 samples from this area. The composition of lithic IRD in these samples reflects regional bedrock composition and forms 38 distinct clusters, or source groups. The term "source group" refers to areas of several hundred to thousands of square kilometers, which share the same lithological and geochemical composition [*Darby*, 2003]. For instance, shallow marine sediments in the northwestern Queen Elizabeth Islands contain over 90% quartz and some clastics, whereas similar samples from around Victoria Island contain 30 to 50% carbonates, plus multicolored crystalline rocks and small amounts of quartz. The composition of every sample is then compared to this source data set with discriminant function analysis.

[8] Like a fingerprint, the chemical signature of each Fe oxide grain is traced to one of 38 unique source areas around the Arctic Ocean [*Darby*, 2003; *Darby et al.*, 1997, 2002; *Darby and Bischof*, 1996]. The same 12 element oxides are analyzed by electron microprobe in each grain along with the mineral type (fresh or altered ilmenite, hematite, ilmeno-hematite (exsolved ilmenite in hematite), ferro-ilmenite (exsolved hematite in ilmenite), titanomagnetite, magnetite, magnetite with other exsolved phases, and chromite. Each grain is matched by mineral type using stepwise discriminant function analysis to all of the more than 2000 circum-Arctic compositional source groups to find the closest match [*Darby*, 2003; *Darby et al.*, 2002]. Only B3/P1 grain matches at 0.95 probability of group membership and 0.5 probability of being closer to a source group centroid than the grains comprising the source group are considered a match. An average of 53% (range 25–

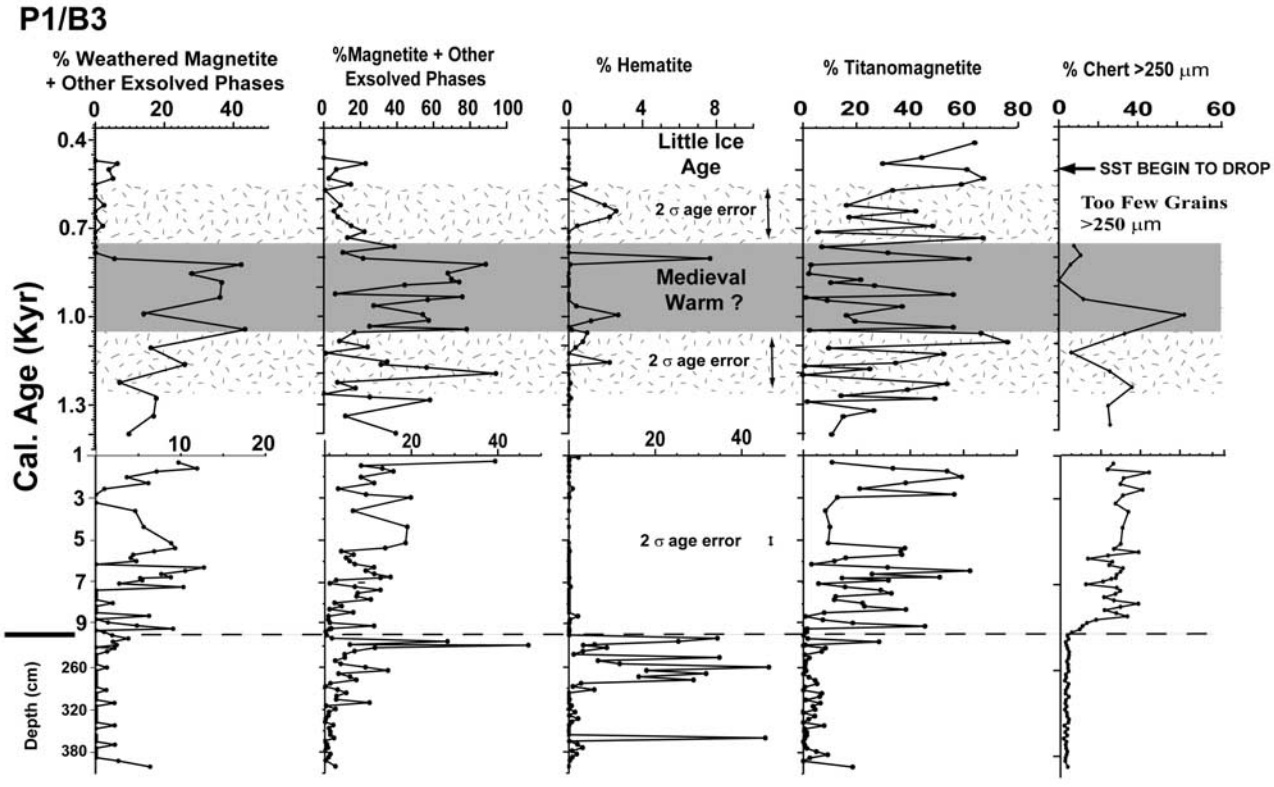

Figure 3. Selected detrital opaque Fe minerals (45–250 μm) and chert (>250 μm) in B3/P1 showing dramatic changes at the last glacial termination (deglaciation) and approximately during the Medieval Warm Period. The abundant mineral, titanomagnetite, fluctuates during the last millennium by significant amounts at a century to subcentury scale. Note the age scale change at 1 ka and the horizontal scale change in the first three minerals at 1 ka. The bottommost data point in the top half of each curve (1.4 ka) is the same as the first point in the lower half. The sea-surface temperature (SST) drop begins as indicated (from *Darby et al.* [2001] and unpublished dinocyst data from A. deVernal).

79%) of the 8,791 analyzed B3/P1 grains matched a source with these conservative criteria, or an average of 43 grains per sample. The minimum level of acceptance for a B3/P1 core sample provenance determination is 10% of matched grains or 5 grains, whichever is greater, matched to a source area [*Darby*, 2003]. Unlike most other provenance tools, this method not only provides a precise source, but the proportion of each source that contributes to a sample. Because of the low numbers of grains matched in some intervals, adjacent depth intervals were combined in these few cases ($n < 25$ grains). This included the uppermost 7 cm in B3 where few sand grains occur.

3. Results: Fe Oxide Mineral Abundances and Sources

[9] There is a significant switch in the types of Fe oxide minerals delivered to the P1 site at about 9.5 kyr BP, i.e., the beginning of the Holocene (Figure 3). Hematite is nearly 40% of the Fe minerals rafted to P1 during the Younger Dryas, but this mineral nearly disappears in the early Holocene. On the other hand, only a few grains of weathered magnetite with exsolved phases and titanomagnetite are ice-rafted to P1 prior to 10 ka. The weathered magnetite increases to nearly 10% and the titanomagnetite to about 50% in the early Holocene. The dominant sources for these and other Fe minerals during the waning stages of the last glacial are the Russian Siberian shelves (~50%) and the northern Canadian ice sheets, the portion of the Laurentide Ice Sheet bordering the Arctic Ocean and the Innuitian Ice Sheet on the Canadian Islands (about 20% each, Figure 4).

[10] Weathered magnetite with other exsolved phases (mostly hematite and ilmenite) occurs above a few percent to 13% in the early Holocene, but it increases to near 40% between 0.8 and 1.1 ka and decreases to less than a few percent since that time. All of these altered magnetite grains contain a few percent SiO_2, suggesting a common source area. Fresh magnetite with other exsolved phases also increases between 0.8 and 1.1 ka. Detrital hematite decreases from near 20% of the Fe oxide minerals to less than 2% from the last glacial to the Holocene. It then increases in the last millennium to a maximum of 8%. Titanomagnetite triples in abundance from the last glacial (7.6% average) to the Holocene (23% average). Most minerals show changes from the last glacial to the Holocene and again in the last millennium that must be due to source changes, either in entrainment at the source or dispersal from the source to this core site. Hematite is more than 20%

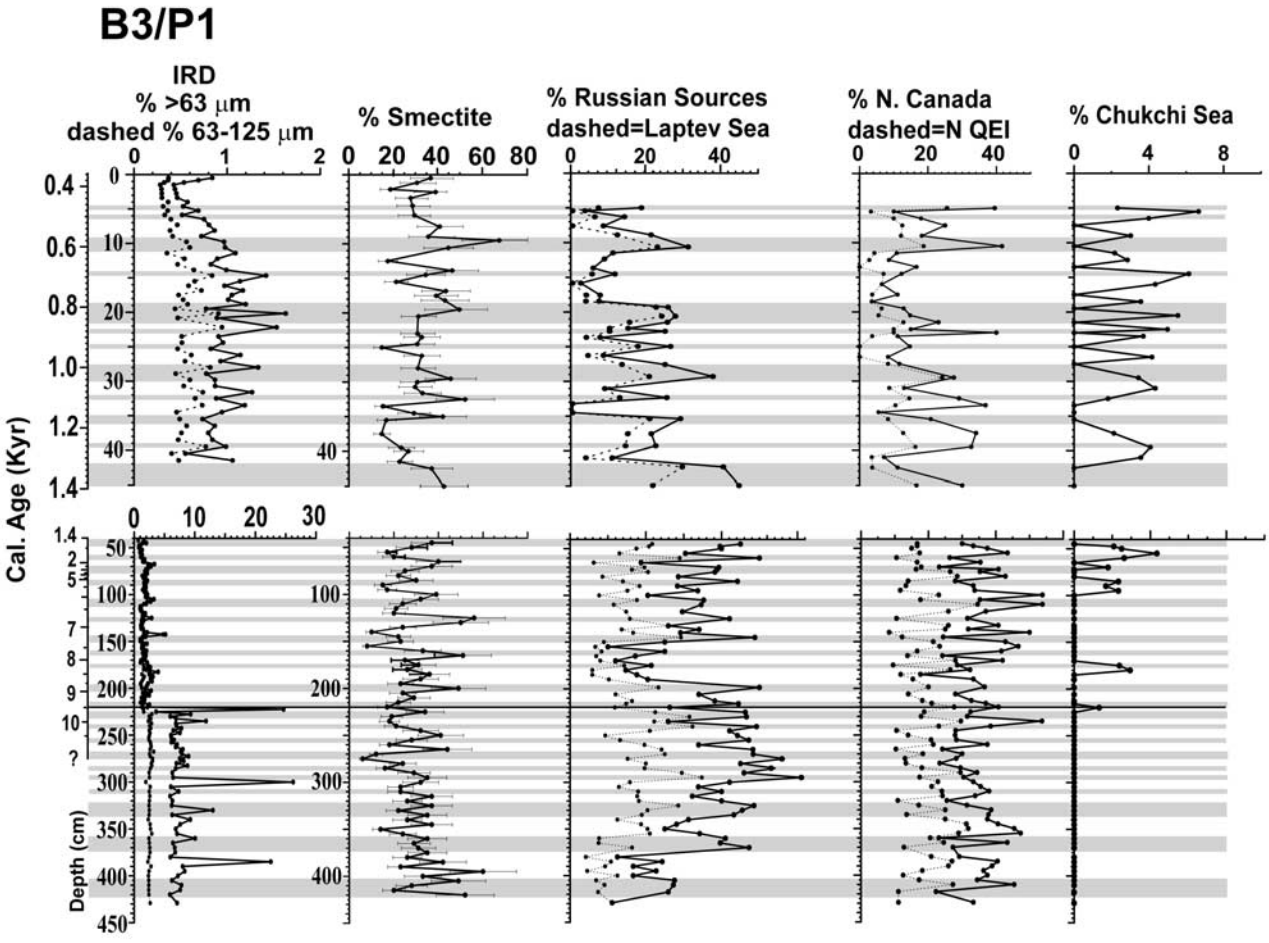

Figure 4. Sand and coarser fractions, smectite clay with ±25% confidence intervals, and Fe grains matched to Russian (Kara Sea to east Siberian Sea) and northern Canadian source areas. Shaded intervals are centered on the Russian Fe grain peaks. The Chukchi grain matches indicate sources immediately south of the core location due to northward drift from the Bering Straits and show very little input from this area. The age scale changes at 1.4 ka and there is a marked decline in sand-sized IRD at the end of the last deglaciation (9.5 kyr).

in several widely separated circum-Arctic source areas, for example, Yenisey River, Laptev Sea, Mackenzie River, and Banks/Victoria Islands. The same is true for the other minerals, which complicates provenance interpretation based solely on these mineral abundances.

[11] The abundances of chert in the >250 μm fraction shows parallel changes with the Fe minerals, increasing dramatically after the last glacial termination and diminishing at the beginning of the Medieval Warm (Figure 3). Chert reaches abundances greater than 60% of the coarse fraction in the Holocene. The only source with this much chert is the DeLong Mountains of northwestern Alaska and adjacent areas of the Chukchi Shelf where rivers from these mountains deposited this chert. Source area samples from other chert-bearing sites never contain more than a few percent chert. While concentration during transport is possible, sampling of dirty ice and bottom sediment thus far has failed to detect such concentrations except in northern Alaska.

[12] The percent smectite in the <2 μm fraction of B3/P1 changes rapidly by more than 20–40% in a quasiperiodic fashion throughout most of the Holocene and the end of the last glacial interval (Figure 4). Abundant smectite clay generally reflects volcanic source rocks. In the Arctic, values of more than 25% are found primarily in the Taymyr Peninsula (western Laptev Sea, Yenisey River areas) [*Pfirman et al.*, 1997; *Dethleff et al.*, 2000; *Ruikka and Strand*, 2002]. But at the P1 core site, high smectite values can also come from volcanic terranes in Chukotka Province of eastern Siberia or southwestern Alaska. In fact, smectite is traced from Alaskan rivers, primarily the Yukon River, into the Arctic Ocean [*Naidu and Mowatt*, 1983]. The rapid fluctuations in smectite abundance suggest changes in sources. Because of the distances from the Laptev Sea, this implies a changing sea ice drift to the P1 site. Several floes contain low to moderate amounts of smectite [*Nürnberg et al.*, 1994; *Cooper et al.*, 1998]. Most of the <2 μm clay fraction would settle-out if transported in

suspension over distances of a few hundred kilometers, especially in the flocculated state typical of marine clays, even at low concentrations [*Ozturgut and Lavelle*, 1986]. Resuspension and transport by bottom currents is unlikely because of the intervening Mendeleev Ridge and the low content of smectite in bottom sediments on the East Siberian Shelf [*Viscosi-Shirley et al.*, 2003a, 2003b]. In the case of the transport from the south through the Bering Strait, surface currents might be strong enough to transport clay and smectite percentages in the <2 μm fraction is occasionally above 25% in the Chukchi Sea [*Viscosi-Shirley et al.*, 2003a]. The shallowness of the Chukchi Sea (mostly <60 m) results in similar suspended transport and sea ice drift. The important question is whether the source of elevated smectite in B3/P1 is the Laptev Sea or the Alaskan/Chukchi Sea area. To answer this question, the ice-rafted Fe oxide grains can provide more definitive answers.

[13] A large number of these Fe grains can be traced to the Euro-Russian Siberian shelves (Fram Strait to Chukchi Sea), mostly the Laptev Sea, particularly during the last millennium (Figure 4). These Russian Fe grains are nearly always present in B3/P1 and average 38% (and up to 63%) of the matched Fe grains. The other major source is northern Canada, primarily the northern Queen Elizabeth Islands (shelf and coastal areas from Ellesmere Island to Ellef Ringnes Island) and the Banks and Victoria Islands area. This northern Canadian source comprises 4 to 54% (average 30%) in B3/P1. Large amounts of glacial sediment were delivered to these coastal and offshore areas during glacial intervals [*Bischof and Darby*, 1999; *Dyke*, 1987]. These sediments are subsequently entrained by sea ice on the shallow shelves and nearshore areas of these Canadian islands during the Holocene [*Darby*, 2003].

4. Discussion

4.1. Glacial to Interglacial IRD Change

[14] The notable changes in Fe mineral types and abundance as well as coarse chert abundance at the termination of the last glacial at about 9.5 kyr BP in B3/P1 reflect a change in sources and/or a change in ice drift. Not only does the IRD abundance drop suddenly at this transition, but also the size of the sand decreases to mostly less than 125 μm except for a few coarser grains in some intervals of the core (Figure 4). This reflects the decrease in IRD from glacial sources where entrainment does not usually exclude coarser grains like sea ice entrainment [*Reimnitz et al.*, 1998]. Only fast ice can routinely entrain coarse grains, even gravel, and occasionally this ice can be floated and blown offshore where its sediment load can become part of the pack ice. Small amounts of >250 μm sediment in P1/B3 throughout the Holocene suggests that this has occurred periodically (Figure 4).

[15] While the Fe minerals suggest a dramatic source change at the glacial/Holocene boundary, the Fe grains matched to potential circum-Arctic source areas indicate little change in sources. Three possible explanations for this are:

[16] 1. Combining most Russian sources and northern Canadian sources obscures source changes across the glacial/Holocene boundary. Of the 38 circum-Arctic source areas (see *Darby et al.* [2002] for map of source areas) 12 distinct areas from the Kara Sea to the eastern Siberian Sea are combined in the Russian sources (Figure 4), and there are enough differences among these sources to account for much of the mineralogical changes.

[17] 2. Some glaciated shelves are also important sites of sea ice entrainment, such as Banks Island [*Darby*, 2003]. Thus, as the transition from glacial to sea ice transport occurred, the sources changed from land areas to different parts of the Siberian or northern Canadian shelves, but still within the same large source areas.

[18] 3. Fe minerals can be size-dependent, changing with the texture of the IRD. The sources might be the same for these different minerals. Thus as IRD texture changed from iceberg IRD (coarser) to sea ice IRD, the mineralogy changed. Yet, there is sufficient overlap in the grain sizes of the different Fe minerals that size alone cannot account for the changes noted from glacial to interglacial.

[19] The abundance of Russian sources, especially the Laptev Sea prior to the Holocene indicates that sea ice-rafting was important even prior to the Holocene. This Russian area was exposed during the last glacial interval but not glaciated [*Bauch et al.*, 2001b]. Only the Barents and Kara Sea areas were covered by ice [*Arkhipov et al.*, 1986; *Mangerud et al.*, 2001]. Any pre-Holocene sediment in B3/P1 from the unglaciated Laptev Sea or east Siberian Sea must have been entrained by sea ice either along the submerged margins of the shelves or by erosion onto the pack ice by wind or runoff [*Muller and Stein*, 2000]. These two large shelf areas constitute the bulk of the Russian Fe grains in B3/P1 throughout the core. Nearly half of the sediment at the end of the Late Pleistocene (prior to 9.5 ka) appears to be from Russian shelves that were not glaciated and thus was transported to B3/P1 via sea ice. The largest source of hematite grains during this time was the eastern Laptev Sea, probably the Lena River. This mineral is always more abundant in the source area rivers than the coastal or shelf areas because it is the most easily weathered Fe mineral of those analyzed [*Darby and Tsang*, 1987]. Thus the Lena River was contributing some sediment to the Arctic Ocean during the last deglaciation despite the fact that it was not glaciated and did not drain a glaciated area.

[20] The northern Canadian Fe grains during the last deglaciation (>9.5 ka) are nearly equally matched to the northern Queen Elizabeth Islands and Banks/Victoria Islands. These sources represent the Innuitian Ice Sheet and Arctic Ocean portion of the Laurentide Ice Sheet, respectively [*Prest*, 1984; *Dyke*, 1987; *England*, 1998; *Bischof and Darby*, 1999; *Darby et al.*, 2002]. While sea ice-rafting cannot be ruled out for these sources during the pre-Holocene, the dominance of land sources as opposed to shelf sources, the coincidence of glacial ice sheet disintegration at this time, and the coarser nature of the sand strongly favor iceberg rafting.

[21] The northern Alaska shelf (not shown in Figure 4) and the Chukchi Sea contributed fewer than 3% Fe grain matches during the pre-Holocene in B3/P1. This is far below the threshold of significance of 8–10% and suggests that fluvial and wind erosion of these unglaciated exposed

shelf areas were not delivering much sediment to the pack ice that could be rafted to the P1 site or eroded from the adjacent Chukchi shelf. This is supported by the low percentage of chert in the coarse lithic fraction at this time. The Chukchi Sea source increases once sea level rose sufficiently to flood this shallow shelf and allow Pacific Ocean water to flow into the Arctic and across the Chukchi Sea. The contribution of Fe grains from this area never exceeds 8% in the Holocene. This is surprising considering that the chert content of the Holocene section alone places its origin firmly in the vicinity of coastal northwest Alaska (67°–69°N). The coarse chert grains were probably transported to P1 by nearshore fastice that was refloated from Alaska, but this shoreline was not sampled for Fe oxide minerals. Thus Fe grains could not be matched to this potential source. This shore ice did not drift directly northwest to P1 because this portion of the Chukchi Sea is sampled and characterized for Fe grain compositions and certainly some shore ice would melt-out along the drift path. Instead, the shore ice must have drifted north along the Alaskan coast with the Alaskan Coastal Current toward Barrow Canyon and then west to the P1 core site.

[22] If a source of Fe grains was south of Bering Strait, ice melt-out should deposit sediment from sea ice moving north through these straits on the Chukchi seafloor. The Fe grains collected from this seafloor and used to characterize this potential source area should then match grains entrained from the Bearing Sea south of the straits. If this assumption is true, then southwestern Alaska is not an important source of Fe grains in B3/P1. Of course, sediment transported by the inflowing Pacific waters might be diverted west toward Herald Canyon, north of Wrangel Island and miss the P1 site (see small dashed arrows in Figure 1) [*Smith et al.*, 2003; *Weingartner et al.*, 1999]. Likewise, there are few Fe grains in B3/P1 from the Beaufort Sea shelf along Alaska to the Mackenzie River. Only a few peaks above 10% in grains from the Mackenzie area occur in the interval 5–9 ka [*Darby et al.*, 2001]. Of the remaining circum-Arctic source areas, only significant grain matches occur from the more southerly Queen Elizabeth Islands that do not border the Arctic Ocean. The percentage from these islands is rarely above the significance threshold of 8–10% in the Holocene but is as high as 22% prior to 10 ka when glacial transport in these islands was north to the Arctic Ocean [*Bischof and Darby*, 1999].

4.2. Submillennial IRD Changes

[23] Because sedimentation rates affect the resolution of frequencies in any time series, IRD fluctuations for the high and constant sedimentation rates during the last 1300 years in P1/B3 provide the best window to past IRD changes at the submillennial scale (Figures 3 and 4). The abundance of weathered magnetite with exsolved phases (WMEP) increases from 16% to 44% around 1100 years BP. Because of the error involved in radiocarbon ages, this is probably near the Medieval Warm period [*Hughes and Diaz*, 1994; *Crowley*, 2000]. This source suddenly diminishes around 800 years BP, perhaps near the start of the Little Ice Age. The total magnetite with exsolved phases (TMEP) shows a sudden decrease and hematite grains spike in abundance at this time (Figure 3). The percentage of Russian Fe grains show a corresponding increase and decline with these magnetite grains, but only the Yenisey River (21% TMEP, 0% WMEP), Yermack Plateau (36% TMEP, 6% WMEP), and the New Siberian Island source areas (6% TMEP, 0% WMEP) have appreciable quantities of this mineral among all the Russian sources. None of these have appreciable amounts of the WMEP. The Chukchi Sea source contains about 10% TMEP and 1–4% WMEP and several sources in the QEI and northern Greenland contain 9–18% TMEP and 3–8% WMEP. Unfortunately, Fe grain fingerprinting of these northern Canadian sources shows a decline to zero grains from these sources during part of the interval in which the TMEP and WMEP grains are highest. None of the 38 characterized source areas and 308 source samples contain more than 10% WMEP grains, and the interval labeled as Medieval Warm in B3/P1 has over 20% WMEP. Thus the precise source of the WMEP grains has not been sampled.

[24] While there is a temptation to causally link the appearance of weathered Fe minerals and a warmer climate in the Medieval Warm interval, a more likely explanation is a change in the atmospheric pressure system and a resultant wind pattern change that would cause sea ice entrainment in different areas than before. This is favored by the fact that nonweathered minerals change at this time, also. Any temperature change during this short interval was unlikely to be large and prolonged enough to initiate significant weathering.

[25] Nearly all peaks of total Russian grains in B3/P1 show rapid fluctuations of 20–30% during the last millennium where sample frequency is 1 cm (Figure 4). These peaks occur approximately every 50–150 years during this time interval and correspond to times when the TPD delivered more grains than usual to the P1 site. Similar high-frequency oscillations might be present earlier in the record, but cannot be resolved with the sampling interval used below 50 cm core depth.

[26] There are two possible drift paths for sea ice delivery of Siberian grains to B3/P1 and both involve a change in the TPD in which it moves closer to North America (Figure 1). This requires a dominant cyclonic flow regime in the Arctic as occurs today during a positive AO [*Kwok*, 2000]. The first drift path is via the TPD deep into the western Arctic, where some TPD ice is diverted south into a restricted or shrunken Beaufort Gyre as the main TPD flows toward Fram Strait. A subsequent switch to a more negative AO would strengthen the Beaufort Gyre and enhance the likelihood of captured Russian ice delivery to the P1 core site. This scenario would favor coincident peaks of northern Canadian Fe grain sources and Russian grain sources at the P1 site. This occurs for slightly more than half of the Russian grain peaks during the last 1300 years (Figure 4). The second drift scenario also involves the TPD expanding eastward even closer to North America and direct transport to the P1 site. This latter drift path requires a very weak Beaufort Gyre and would favor Russian grain peaks without input from North America. Today, this scenario only rarely occurs when the AO index is above +2 [*Kwok*, 2000; *Rigor et al.*, 2002]. Regardless of which scenario operates,

increases in Russian Fe grains at B3/P1 indicate a shift in the TPD toward Alaska analogous to what has been shown in various ocean models and observations of the ice drift during a positive Arctic Oscillation (AO+; Figure 1) [*Kwok*, 2000; *Rigor et al.*, 2002; *Mysak*, 2001; *Proshutinsky and Johnson*, 1997, 2001; *Dickson et al.*, 2000].

[27] The Russian Fe grain peaks correspond to >25–30% smectite clay (r = 0.5) suggesting that the Russian sources also contain high amounts of this clay mineral. As previously noted, smectite in abundances above 25–30% can be traced to either the Laptev Sea area or the Chukchi and Beringa area. Based on the results of Fe grain matches and assuming that most of the clay is transported by sea ice, the Laptev area seems to be a more probable source. The few instances where Russian sources are low and smectite is high indicate that during these occasions, the smectite is derived from south of P1. The rare occasions when Russian Fe grain sources are high and smectite is low are due to Russian sources other than the Laptev Sea, primarily the east Siberian Sea.

[28] Previous papers using contaminants [*Smith et al.*, 2003; *Gobeil et al.*, 2001], driftwood [*Tremblay et al.*, 1997], and Fe grain matches [*Darby*, 2003] of Siberian sediment in the Beaufort Gyre are evidence suggesting that Russian sediment is frequently transported to the Beaufort Sea. *Tremblay et al.* [1997] first proposed the concept of an expanded TPD as the cause of the Russian driftwood in northern Canada. Core B3/P1 presents further evidence supporting the drift of Russian sediment to the P1 site as a fairly regularly occurring phenomenon during, and even before the Holocene.

[29] The frequency of incursions of the Russian grains and, therefore, the expansion of the TPD toward North America and into the Beaufort Gyre appears to be multidecadal during the last 1300 years (Figure 4). The frequency varies from about half a century to somewhat more than a century during this time. This pattern of prolonged time intervals of several decades where Russian grains are delivered to the P1 site in high amounts is very similar to the pattern of multidecadal intervals where the Arctic Oscillation is either positive or negative. For example, there is a prolonged interval of fluctuating negative AO (mean vorticity index) [*Walsh et al.*, 1996] from 1960–1980 [*Mysak*, 2001] and the highly correlated North Atlantic Oscillation (NAO) was generally positive from 1830 to 1950 AD (winter NAO) [*Luterbacher et al.*, 2001] based on reconstructions from paleoclimate data. Thus while the AO and NAO have periodicities of a decade or less [e.g., *Hurrell*, 1995], they also have a more complex longer time periodicity on a submillennial scale and perhaps a multidecadal scale.

[30] The sedimentation rates in P1 during the middle Holocene are too low and the sampling interval too large to determine submillennium frequencies in the data. There are 11 peaks in the percentage of Russian Fe grains in B3/P1 between 1.3 and 9.5 ka (shaded intervals, Figure 4). Similar variations occur prior to 9.5 ka during the deglaciation. Because the age model for P1 lacks measurements older than 7 ka, and since the entire interval older than about 9 ka might be less than a thousand years, no interpretation is possible for this older interval. Russian grains occurring in the deglacial sediment (>9.5 ka) indicate that an expanded TPD occurred at this time to deliver them to the P1 site. Thus the atmospheric forcing that caused the change in the TPD operated as far back as the deglaciation of the last glacial interval.

5. Conclusions

[31] The detrital Fe oxide mineral grains analyzed in core B3/P1 provide additional evidence of the influx of sand-size sediment from Russian shelves into the North American shelf area and the Beaufort Gyre. These grains were ice-rafted by sea ice and the amount of input fluctuated on a century to subcentury timescale during the last millennium and probably throughout the Holocene. This oscillating influx is best explained by an expanded TPD that moves closer to North America and either directly delivers sediment-laden ice from Russian shelves to the P1 core site on the edge of the Chukchi Sea or delivers large amounts of this ice to the Beaufort Gyre, which in turn delivers it to the P1 site. This periodically expanded TPD circulation pattern has operated since at least the time of the last deglaciation (~9–11 kyr BP). The close correlation between the NAO and AO means that not only can we conclude that the AO is a long-term component of the climate system, but that the same is true for the NAO. The large changes in chert and detrital Fe minerals in the IRD at the last termination and again near the Medieval Warm/Little Ice Age suggest that these climatic events influenced or are associated with changes in pack ice drift and/or sources of sea ice IRD.

[32] **Acknowledgments.** This work was supported by NSF grants OPP-9817051 and OPP-0136171. We thank L. Phillips and the USGS for the core material the use of the core sampling facilities at Menlo Park. Earlier versions of this paper were improved upon by suggestions from L. Polyak and three anonymous reviewers.

References

Aagaard, K., and E. Carmack (1989), The role of sea ice and other fresh water in the Arctic circulation, *J. Geophys. Res.*, *94*, 14,485–14,498.

Arkhipov, S. A., V. G. Bespaly, M. A. Faustova, O. Glushkova, L. L. Isayeva, and A. A. Velichko (1986), Ice sheet reconstructions, *Quat. Sci. Rev.*, *5*, 475–483.

Bauch, H. A., H. Kassens, O. D. Naidina, M. Kunz-Pirrung, and J. Thiede (2001a), Composition and flux of Holocene sediments on the eastern Laptev Sea shelf, Arctic Siberia, *Quat. Res.*, *55*, 344–351.

Bauch, H. A., T. Mueller-Lupp, E. Taldenkova, R. F. Spielhagen, H. Kassens, P. M. Grootes, J. Thiede, J. Heinemeier, and V. V. Petryashov (2001b), Chronology of the Holocene transgression at the North Siberian margin, *Global Planet. Change*, *31*, 125–140.

Bischof, J., and D. A. Darby (1999), Quaternary ice transport in the Canadian Arctic and extent of Late Wisconsinan glaciation in the Queen Elizabeth Islands, *Can. J. Earth Sci.*, *36*, 2007–2022.

Cooper, L. W., I. L. Larsen, T. M. Beasley, S. S. Dolvin, J. M. Grebmeier, J. M. Kelley, M. Scott, and A. Johnson-Pyrtle (1998), The distribution of radiocesium and plutonium in sea ice-entrained arctic sediments in relation to potential sources and sinks, *J. Environ. Radioact.*, *39*(3), 279–303.

Crowley, T. J. (2000), Causes of climate change over the past 1000 years, *Science*, *289*, 270–277.

Darby, D. A. (2003), Sources of sediment found in sea ice from the western Arctic Ocean: New insights into processes of entrainment and drift patterns, *J. Geophys. Res.*, *108*(C8), 3257, doi:10.1029/2002JC001350.

Darby, D. A., and J. F. Bischof (1996), A statistical approach to source determination of lithic and Fe-oxide grains: An example from the Alpha Ridge, Arctic Ocean, *J. Sediment. Res.*, *66*(3), 599–607.

Darby, D. A., and Y. W. Tsang (1987), The variation in ilmenite element composition within and among drainage basins: Implications for provenance, *J. Sediment. Petrol.*, *57*(5), 831–838.

Darby, D. A., J. F. Bischof, and G. A. Jones (1997), Radiocarbon chronology of depositional regimes in the western Arctic Ocean, *Deep Sea Res. Part II*, *44*, 1745–1757.

Darby, D., J. Bischof, G. Cutter, A. deVernal, C. Hillaire-Marcel, G. Dwyer, J. McManus, L. Osterman, L. Polyak, and R. Poore (2001), New record of pronounced changes in Arctic Ocean circulation and climate, *Eos Trans. AGU*, *82*(49), 603–607.

Darby, D. A., J. F. Bischof, R. F. Spielhagen, S. A. Marshall, and S. W. Herman (2002), Arctic ice export events and their potential impact on global climate during the late Pleistocene, *Paleoceanography*, *17*(2), 1025, doi:10.1029/2001PA000639.

Delworth, T. L., and K. W. Dixon (2000), Implications of the recent trend in the Arctic/North Atlantic Oscillation for the North Atlantic thermohaline circulation, *J. Clim.*, *13*(21), 3721–3727.

Dethleff, D., V. Rachold, M. Tintelnot, and M. Antonow (2000), Sea-ice transport of riverine particles from the Laptev Sea to Fram Strait based on clay mineral studies, *Int. J. Earth Sci.*, *89*, 496–502.

Dickson, R. R., J. Meincke, S. A. Malmberg, and A. Lee (1988), The "Great Salinity Anomaly" in the North Atlantic 1968–1982, *Prog. Oceanogr.*, *20*, 103–151.

Dickson, R. R., T. J. Osborn, J. W. Hurrell, J. Meincke, J. Blindheim, B. Adlandsvik, T. Vinje, G. Alekseev, and W. Maslowski (2000), The Arctic Ocean response to the North Atlantic Oscillation, *J. Clim.*, *13*(15), 2671–2696.

Dyke, A. S. (1987), A reinterpretation of glacial and marine limits around the northwestern Laurentide Ice Sheet, *Can. J. Earth Sci.*, *24*, 591–601.

England, J. (1998), Support for the Innuitian Ice Sheet in the Canadian High Arctic during the Last Glacial Maximum, *J. Quat. Sci.*, *13*, 275–280.

Forman, S. L., and L. Polyak (1997), Radiocarbon content of pre-bomb marine mollusks and variations in the ^{14}C reservoir age for coastal areas of the Barents and Kara Seas, Russia, *Geophys. Res. Lett.*, *24*, 885–888.

Gobeil, C., R. W. McDonald, J. N. Smith, and L. Beaudin (2001), Atlantic water flow pathways revealed by lead contamination in Arctic Basin sediments, *Science*, *293*, 1301–1304.

Hilmer, M., and T. Jung (2000), Evidence for a recent change in the link between the NAO and Arctic sea ice export, *Geophys. Res. Lett.*, *27*(7), 989–992.

Hughes, M. K., and H. F. Diaz (1994), Was there a Medieval Warm Period, and if so, where and when?, *Clim. Change*, *26*, 109–142.

Hurrell, J. W. (1995), Decadal trends in the North Atlantic oscillation: Regional temperature and precipitation, *Science*, *269*, 676–679.

Kennett, J. P., and E. A. Ingram (1995), A 20,000-year record of ocean circulation and climate change from the Santa Barbara basin, *Nature*, *377*, 323–326.

Kiefer, T., M. Sarnthein, H. Erlenkeuser, P. M. Grootes, and A. P. Roberts (2001), North Pacific response to millennial-scale changes in ocean circulation over the last 60 kyr, *Paleoceanography*, *16*(2), 179–189.

Kwok, R. (2000), Recent changes in Arctic Ocean sea ice motion associated with the NAO, *Geophy. Res. Lett.*, *27*(6), 775–778.

Kwok, R., and D. A. Rothrock (1999), Variability of Fram Strait ice flux and North Atlantic oscillation, *J. Geophys. Res.*, *104*(C3), 5177–5189.

Luterbacker, J., et al. (2001), Extending the North Atlantic Oscillation reconstructions back to 1500, *Atmos. Sci. Lett.*, *2*, 114–124.

Mangerud, J., V. I. Astakhov, A. Murray, and J. I. Svendsen (2001), The chronology of a large ice-damned lake and the Barents-Kara Ice Sheet advances, northern Russia, *Global Planet. Change*, *31*, 321–336.

Muller, C., and R. Stein (2000), Variability of fluvial sediment supply to the Laptev Sea continental margin during the Late Weichselian to Holocene times: Implications from clay-mineral records, *Int. J. Earth Sci.*, *89*, 592–604.

Mysak, L. A. (2001), Patterns of Arctic circulation, *Science*, *293*, 1269–1270.

Mysak, L. A., and S. A. Venegas (1998), Decadal climate oscillations in the Arctic: A new feedback loop for atmospheric-ice-ocean interactions, *Geophys. Res. Lett.*, *25*(19), 3607–3610.

Naidu, A. S., and T. C. Mowatt (1983), Sources and dispersal patterns of clay minerals in surface sediments from the continental shelf areas off Alaska, *Geol. Soc. Am. Bull.*, *94*, 841–854.

Nürnberg, D., I. Wollenburg, D. Dethleff, H. Eicken, H. Kassens, T. Letzig, E. Reimnitz, and J. Thiede (1994), Sediments in Arctic sea ice: Implications for entrainment, transport and release, *Mar. Geol.*, *119*(3–4), 185–214.

Ozturgut, O., and J. W. Lavelle (1986), Settling analysis of fine sediment in salt water at concentrations low enough to preclude flocculation, *Mar. Geol.*, *69*(3–4), 353–362.

Pfirman, S. L., R. Colony, D. Nürnberg, H. Eicken, and I. Rigor (1997), Reconstructing the origin and trajectory of drifting Arctic sea ice, *J. Geophy. Res.*, *102*, 12,575–12,586.

Phillips, R. L., and A. Grantz (1997), Quaternary history of sea ice and paleoclimate in the Amerasia basin, Arctic Ocean, as recorded in the cyclical strata of Northwind Ridge, *Geol. Soc. Am. Bull.*, *109*, 1101–1115.

Poore, R. Z., L. Osterman, W. B. Curry, and R. L. Phillips (1999), Late Pleistocene and Holocene meltwater events in the western Arctic Ocean, *Geology*, *27*(8), 759–762.

Prest, V. K. (1984), The Late Wisconsinan glacier complex, in *Geol. Surv. Can. Pap. 84-10*, edited by R. J. Fulton, pp. 22–36, Dartmouth, Nova Scotia.

Proshutinsky, A., and M. Johnson (1997), Two circulation regimes of the wind driven Arctic Ocean, *J. Geophys. Res.*, *102*, 12,493–12,514.

Proshutinsky, A., and M. Johnson (2001), Two regimes of the Arctic's circulation from ocean models with ice and contaminants, *Mar. Pollut. Bull.*, *43*, 61–70.

Raymo, M. E., D. Rind, and W. F. Ruddiman (1990), Climatic effects of reduced Arctic sea ice limits in the GISS II general circulation model, *Paleoceanography*, *5*, 367–382.

Reimnitz, E., M. McCormick, J. Bischof, and D. A. Darby (1998), Comparing sea-ice sediment load with Beaufort Sea shelf deposits: Is entrainment selective?, *J. Sediment. Res.*, *68*, 777–787.

Rigor, I. G., J. M. Wallace, and R. L. Colony (2002), On the response of sea ice to the Arctic Oscillation, *J. Clim.*, *15*(18), 2648–2668.

Ruikka, M., and K. Strand (2002), Clay minerals in response to the Pleistocene climate change on the Yermak Plateau, Arctic Ocean (ODP, site 911), *Polar Record*, *38*(206), 241–248.

Smith, J. N., S. B. Moran, and R. W. Macdonald (2003), Shelf–basin interactions in the Arctic Ocean based on 210Pb and Ra isotope tracer distributions, *Deep Sea Res. Part I*, *50*(3), 397–416.

Southon, J. R., D. E. Nelson, and J. S. Vogel (1990), A record of past ocean-atmosphere radiocarbon differences from the northeast Pacific, *Paleoceanography*, *5*, 197–206.

Stuiver, M., and P. J. Reimer (1993), Extended ^{14}C data base and revised CALIB 3.0 ^{14}C age calibration program, *Radiocarbon*, *35*, 215–230.

Stuiver, M., P. J. Reimer, E. Bard, J. W. Beck, G. S. Burr, K. A. Hughen, B. Kromer, G. McCormack, J. van der Plicht, and M. Spurk (1998), INTCAL98 radiocarbon age calibration, 24,000–0 cal BP, *Radiocarbon*, *40*, 1041–1083.

Thompson, D. W. J., and J. M. Wallace (1998), The Arctic Oscillation signature in the wintertime geopotential height and temperature fields, *Geophy. Res. Lett.*, *25*(9), 1297–1300.

Tremblay, L. B., L. A. Mysak, and A. S. Dyke (1997), Evidence from driftwood records for century-to-millennium scale variations of the high latitude atmospheric circulation during the Holocene, *Geophys. Res. Lett.*, *24*(16), 2027–2030.

Viscosi-Shirley, C., K. Mammone, N. Pisias, and J. Dymond (2003a), Clay mineralogy and multi-element chemistry of surface sediments on the Siberian-Arctic shelf: Implications for sediment provenance and grain size sorting, *Cont. Shelf Res.*, *23*(11–23), 1175–1200.

Viscosi-Shirley, C., N. Pisias, and K. Mammone (2003b), Sediment source strength, transport pathways and accumulation patterns on the Siberian Arctic's Chukchi and Laptev shelves, *Cont. Shelf Res.*, *23*(11–23), 1201–1225.

Walsh, J. E., W. L. Chapman, and T. L. Shy (1996), Recent decrease of sea level pressure in the central Arctic, *J. Clim.*, *9*(2), 480–485.

Weingartner, T. J., S. Danielson, Y. Sasaki, V. Pavlov, and M. Kulakov (1999), The Siberian Coastal Current: A wind-driven and buoyancy-forced Arctic coastal current, *J. Geophys. Res.*, *104*(C12), 29,697–29,713.

J. F. Bischof and D. A. Darby, Department of Ocean, Earth, and Atmospheric Sciences, Old Dominion University, Norfolk, VA 23529, USA. (ddarby@odu.edu)